

# Effect of fractional blood flow on plasma skimming in the microvasculature

Jiho Yang,<sup>1,2</sup> Sung Sic Yoo,<sup>1</sup> and Tae-Rin Lee<sup>1,\*</sup>

<sup>1</sup>Advanced Institutes of Convergence Technology, Seoul National University, Suwon 443-270, Republic of Korea

<sup>2</sup>Department of Computer Science, Technische Universität München, Boltzmannstraße 3, Garching, Germany

Although redistribution of red blood cells at bifurcated vessels is highly dependent on flow rate, it is still challenging to quantitatively express the dependency of flow rate in plasma skimming due to nonlinear cellular interactions. We suggest a plasma skimming model that can involve the effect of fractional blood flow at each bifurcation point. For validating the new model, it is compared with *in vivo* data at single bifurcation points, as well as microvascular network systems. In the simulation results, the exponential decay of plasma skimming parameter,  $M$ , along fractional flow rate shows the best performance in both cases.

Red blood cells (RBCs) in microvessels are concentrated on the vessel core. Subsequently, a cell-free layer (CFL) with a few micrometer thickness is observed on the vessel wall. The CFL leads asymmetric redistribution of hematocrit at each bifurcations, called plasma skimming effect. As a continuous process of plasma skimming in microvascular networks, the average hematocrit in capillary beds is lower than the systemic hematocrit as reported in many previous studies [1–8]. Interestingly, the plasma skimming is recently revisited to develop new microchannels for detecting specific DNAs, proteins and cells by efficiently separating plasma from whole blood [9–11]. Also, it has been highlighted to accurately predict drug carrier distribution in the microvasculature [12–18]. For utilizing the plasma skimming to new applications *in vitro* and *in vivo*, it is crucial to quantitatively predict the redistribution of RBCs and plasma at bifurcations.

From the early 70s, several experiments for quantifying the plasma skimming were performed [2, 19–23]. As pioneers, Pries et al [24] measured plasma skimming regarding fractional blood flow in two different cases of *in vivo* mouse model. The experiments confirmed previous studies that flow fractionation at the capillary entrance is an important determinant of capillary hematocrit, not the absolute flow velocity itself [2]. Then, the plasma skimming was expressed by Logit model considering fractional flow rate and vessel diameters [25]. This model matches well with previous experimental data at single bifurcations with specific curve fitting parameters. Recently, for improving extensibility of plasma skimming model to various conditions in microvascular networks, Gould and Linninger [26] suggested a new model that can quantify the plasma skimming with a single parameter,  $M$ . Also, Lee *et al.* [16] introduced a generalized version of plasma skimming model for cells and drug carriers.

In this Letter, we aim to mathematically model fractional blood flow in a simple and generalized manner in order to computationally study its significance in plasma skimming, and also to accurately predict plasma skimming in the microvasculature. For this task, a recently developed plasma skimming model [26] is taken, and extended to take into account the effect of fractional blood

flow. This new model is then validated with experimental data at single bifurcation level, and also at microvascular network level.

While there are other plasma skimming models [25, 27], the model developed by Gould and Linninger [26] is considered due to its easy extensibility. The model is as follows:

$$H_1 = H_0 - \Delta H = \zeta_1 H^* \quad (1)$$

$$H_2 = \zeta_2 H^* \quad (2)$$

$$Q_0 H_0 = Q_1 H_1 + Q_2 H_2 = Q_1 \zeta_1 H^* + Q_2 \zeta_2 H^* \quad (3)$$

$$\zeta_i = \left( \frac{A_i}{A_0} \right)^{\frac{1}{M}} \quad \text{where } i = 1, 2 \quad (4)$$

where  $H$  is the hematocrit,  $M$  is the plasma skimming parameter,  $\zeta$  is the hematocrit change coefficient due to plasma skimming,  $Q$  is the flow rate,  $A$  is the cross-sectional area of each vessel, and subscript 0, 1, and 2 indicate the parent, and two daughter vessels, respectively. Specifically, the plasma skimming parameter  $M$  reflects the cross-sectional distribution of RBCs. Small  $M$  represents that RBCs are highly concentrated on the vessel core. In other words, plasma dominant region, or CFL, is developed on the near wall region. The two separated regions, expressed as RBCs and plasma areas, lead to strong plasma skimming. On the contrary, high  $M$  means well-mixed RBCs and plasma. As a result, the plasma skimming effect will be diminished. Although plasma skimming is a function of hemodynamic parameters,  $M$  was fixed at a constant value,  $M = 5.25$ , for the entire microvasculature [26] due to its complexity.

Here, for improving the plasma skimming model, the flow rate change from parent to daughter vessels is expressed by

$$M = M_0 \cdot e^{-k \frac{Q_1}{Q_0}} \quad (5)$$

where  $M_0$  and  $k$  are constant values for quantifying  $M$  as a function of fractional blood flow. In our simulation,  $M_0$  and  $k$  are 10 and 4, respectively. Note that the subscript 1 denotes the daughter vessel with the largest

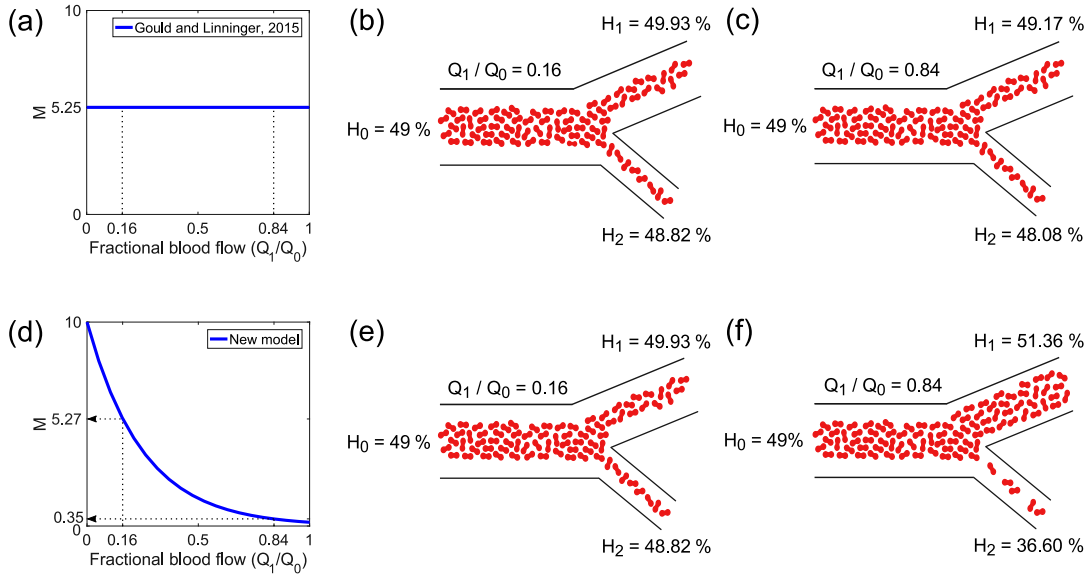


FIG. 1. Plots of plasma skimming parameter  $M$  against fractional blood flow, and illustrations of RBC redistribution in two cases.  $Q_1/Q_0$  denotes the fractional blood flow between the largest daughter vessel and parent vessel. Without using the fractional blood flow model (a-c) there is negligible change in RBC redistributions at bifurcation since  $M$  is set as a constant. When including the effect of fractional blood flow (d-f), both hemoconcentration and hemodilution after plasma skimming become more significant.

diameter. The exponential decay function of  $M$  weakens the plasma skimming at low  $Q_1/Q_0$  and vice versa. For instance, when  $Q_1/Q_0$  is reduced, the natural flow tendency from parent vessel to daughter vessel with larger diameter is disturbed and then well-mixed at the bifurcation point. Under such circumstance, the hematocrit change from plasma skimming is small. On the other hand, at high  $Q_1/Q_0$ , the natural flow with CFL from parent vessel is prolonged to daughter vessel with larger diameter, leading to hematocrit redistribution.

Figure 1 depicts plots of  $M$  against fractional blood flow and schematic illustrations of RBC redistribution with computed hematocrit values with and without fractional blood flow model at single bifurcation. For this computation, hematocrit value at parent vessel is set to 49% and diameters of parent, and two daughter vessels are set to  $20\mu\text{m}$ ,  $17.5\mu\text{m}$ , and  $16.5\mu\text{m}$ , respectively. Figure 1(a) shows the plot of  $M$  over fractional blood flow when  $M$  is set as a constant [26]. Figure 1(b) and (c) show the RBC redistributions when  $Q_1/Q_0$  is 0.16 and 0.84, respectively. Since no relationship between the plasma skimming parameter and fractional blood flow was established in the original model,  $M$  remains as a constant. In this case, change in RBC redistribution when varying  $Q_1/Q_0$ , for a given parent vessel hematocrit, is negligible.

Figure 1(d) represents the plot of  $M$  when Eq.(5) is applied. As shown in Fig.1(e), the hematocrit change at  $Q_1/Q_0 = 0.16$  is similar to that in Fig.1(b) due to the similar  $M$  values. However, as described previously, increment in fractional blood flow produces greater plasma

skimming, and hence  $M$  is reduced. When  $Q_1/Q_0$  is 0.84,  $M$  now becomes 0.35. As depicted in Fig.1(f), rather significant change is observed in RBC redistribution compared with Fig.1(c), where the difference in hematocrit between the daughter vessels becomes more significant. By considering the effect of fractional blood flow, both hemoconcentration and hemodilution in the daughter vessels are amplified. Equation (5) with corresponding constants, as stated previously, is the only equation applied to model the effect of fractional blood flow.

In order to validate the fractional blood flow model, plasma skimming at single bifurcation is computed and compared with *in vivo* experimental data [24], along with the model developed by Gould and Linninger [26]. Logit model [24, 25] is not considered for single bifurcation since this model was developed based on curve fitting of the same experimental data [24]. The physiological conditions as observed in the experiment are considered, and this is summarized in Tab.I.  $H_0$  denotes hematocrit value at parent vessel, and  $d_0$ ,  $d_1$ , and  $d_2$  denote diameters of parent vessel, and two daughter vessels, respectively. The same fractional model of Eq.(5) is used for both geometries.

Figure. 2 depicts the ratio of hematocrit,  $H_i/H_0$ , for two geometry cases from Tab.I. The fractional blood flow model matches very well with the experimental data, particularly in Fig.2(b). While the model developed by Gould and Linninger [26] does not sufficiently capture hemoconcentration and hemodilution, fractional blood flow model significantly amplifies them.  $H_1$  from frac-

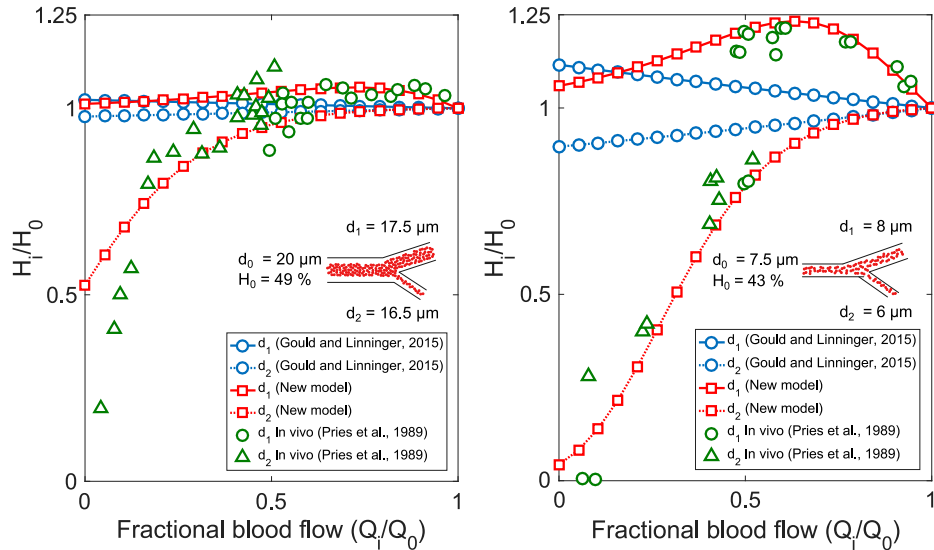


FIG. 2. Ratio of hematocrit between parent and daughter vessels ( $H_i/H_0$ ) against fractional blood flow ( $Q_i/Q_0$ ) at single bifurcation for comparing fractional blood flow model with the model developed by Gould and Linninger [26] and experimental data [24]. Two cases of geometries stated in Tab.I are considered. Significant amplifications in both hemoconcentration and hemodilution are produced by using fractional blood flow model, accurately matching with the experimental data.

TABLE I. Physiological conditions used for validation of fractional blood flow model at single bifurcation

Case	$H_0$	$d_0$	$d_1$	$d_2$
1	49%	20 $\mu\text{m}$	17.5 $\mu\text{m}$	16.5 $\mu\text{m}$
2	43%	7.5 $\mu\text{m}$	8 $\mu\text{m}$	6 $\mu\text{m}$

tional blood flow model on Fig.2(b), for instance, increases up to 1.25 showing significant hemoconcentration. Similarly,  $H_2$  from fractional blood flow model shows very significant hemodilution down to 0.04 as  $Q_2/Q_0$  decreases.

To predict the plasma skimming effect at microvascular network level, the fractional blood flow model is coupled with mathematical model of blood flow. A microvascular network model is computationally generated based on mathematical algorithms by choosing vessel diameter ( $d_i$ ), vessel length ( $l_i$ ), and bifurcation angles ( $\theta_i$  and  $\phi_i$ ) [16, 30]. Diameters of daughter vessels at each bifurcation are governed by  $d_0^\gamma = d_1^\gamma + d_2^\gamma$  where  $\gamma$  is fixed at 3 [31, 32]. Ratio of two daughter vessels,  $\eta = d_2/d_1$ , is utilized to control the geometric asymmetry of the entire microvascular network. With the diameter ratio,  $\eta$ , the diameters of daughter vessels are described by  $d_1 = \sqrt[\gamma]{d_0^\gamma / (1 + N(\eta, \sigma^2)^\gamma)}$  and  $d_2 = \sqrt[\gamma]{d_0^\gamma - d_1^\gamma}$  where  $N$  is a normal distribution with mean  $\eta = 0.62$  and standard deviation  $\sigma = 0.1$  for capturing the heterogeneous diameter distribution.

The diameter of root vessel is set to 40 $\mu\text{m}$  and cut-off diameter is set to 6 $\mu\text{m}$ . Vessel lengths are governed by  $l_i = \beta d_i^n$  where  $\beta$  is 100 and  $n$  is 0.46. Pressure

drops between the root vessel and the capillary ends are 47mmHg. Flow rates of blood flow ( $Q_i$ ) is calculated by Poiseuille flow model, conservation of mass and *in vivo* viscosity laws [33] with the reference viscosity of plasma, fixed at  $9 \cdot 10^{-6}$  mmHg·s [34]. To express the variation of systemic hematocrit, the initial hematocrit values have a range from 0.3 to 0.5. The plasma skimming is controlled by considering CFL thickness in the plasma skimming model as  $M' = M(1 + 15 \exp(1 - \delta'/0.03))$  where  $\delta'$  is the relative CFL with respect to vessel diameter. For the validation of fractional blood flow model, two other plasma skimming models are considered for comparison: Logit model [25] and the model developed by Gould and Linninger [26].

Figure 3 depicts the computationally generated microvasculature model. Systemic hematocrit of 45% is applied as an initial boundary condition. Figure 3(a) shows the microvasculature geometry used for predicting plasma skimming at microvascular network level. Figure 3(b) and (c) are the flow velocity and pressure with respect to vessel diameters, respectively. As plotted in the figures, the mathematical model considering the effect of fractional blood flow holds good agreement with *in vivo* data [28, 29].

Figure 4 shows the hematocrit distribution along with vessel diameters. Three models, Logit model, Gould and Linninger's model and the fractional flow model, are compared with *in vivo* hematocrit scatter data [35]. All three models capture the plasma skimming in capillary beds. However, the Logit and Gould and Linninger's models require an artificial cut-off value of hematocrit due to the early hemoconcentration between 20 and 40 $\mu\text{m}$  vessel di-

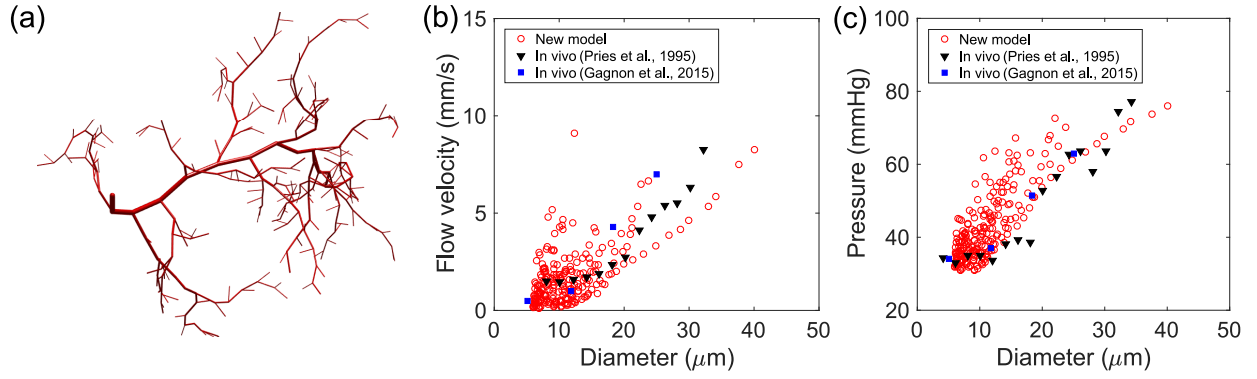


FIG. 3. Computational model of microvascular network and corresponding hemodynamic calculations. Vessel diameters are asymmetrically decreased from  $40$  to  $6\mu\text{m}$ . The pressure drop between the root vessel to capillary ends is set to  $47\text{mmHg}$ . The simulation results are compared with two *in vivo* experimental data [28, 29]. (a) microvascular geometry, (b) flow velocity distribution and (c) pressure distribution.

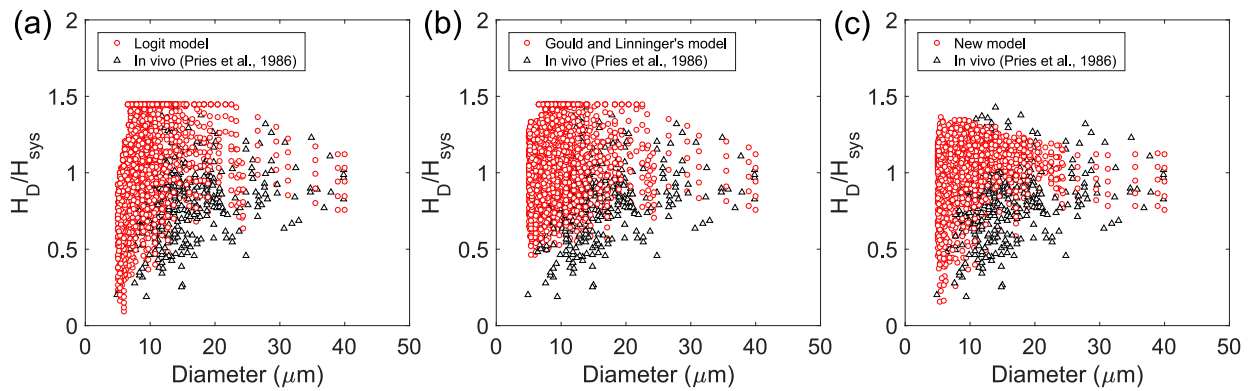


FIG. 4. Relative hematocrit distribution along with vessel diameters at the microvascular network model. The systemic hematocrit,  $H_{sys}$ , is set to  $0.45$ . Black triangle marks represent *in vivo* experimental data [35]. The initial hematocrit at the root vessel is varied from  $0.3$  to  $0.5$ . (a) Logit model (b) Gould and Linninger's model (c) Fractional flow model.

ameters. Unlike these two models, with the new model considering fractional blood flow, the plasma skimming is started when the vessel diameter is below  $20\mu\text{m}$  without applying the cut-off hematocrit value. Moreover, the computed hematocrit values in the given microvascular geometry is smoothly dispersed in the range from  $6$  to  $40\mu\text{m}$  vessel diameters.

In conclusion, for the first time, the effect of fractional blood flow on plasma skimming of RBCs in the microvasculature is mathematically designed, and quantitatively predicted. As shown from the results, fractional blood flow model accurately matches with *in vivo* experimental data, at both single bifurcation and microvascular network level, indicating that fractional blood flow is an important parameter that must be taken into account for studying plasma skimming. Furthermore, these results quantitatively validate previous qualitative and experimental studies that fractional blood flow greatly affects plasma skimming.

This research was supported by Basic Science Research Program through the National Research Foundation of

Korea (NRF) funded by the Ministry of Education (NRF-2015R1D1A1A01060992), and by the Bio and Medical Technology Development Program of the National Research Foundation (NRF) funded by the Ministry of Science, ICT and Future Planning (2016M3A9B4919711).

\* Corresponding author, taerinlee@snu.ac.kr

- [1] J. Cohnstein and N. Zuntz, Pflügers Archiv European Journal of Physiology **42**, 303 (1888).
- [2] P. C. Johnson, J. Blaschke, K. S. Burton, and J. Dial, American Journal of Physiology—Legacy Content **221**, 105 (1971).
- [3] G. Schmid-Schoenbein and B. Zweifach, Microvascular research **10**, 153 (1975).
- [4] B. Klitzman and B. R. Duling, American Journal of Physiology—Heart and Circulatory Physiology **237**, H481 (1979).
- [5] H. H. Lipowsky, S. Usami, and S. Chien, Microvascular research **19**, 297 (1980).
- [6] G. Kanzow, A. R. Pries, and P. Gaehtgens, Bibl. Anat.

- 20, 149 (1981).
- [7] G. Kanzow, A. Pries, and P. Gaehtgens, International journal of microcirculation, clinical and experimental/sponsored by the European Society for Microcirculation **1**, 67 (1982).
- [8] I. H. Sarelius, D. N. Damon, and B. R. Duling, American Journal of Physiology-Heart and Circulatory Physiology **241**, H317 (1981).
- [9] R. Fan, O. Vermesh, A. Srivastava, B. K. Yen, L. Qin, H. Ahmad, G. A. Kwong, C.-C. Liu, J. Gould, L. Hood, *et al.*, Nature biotechnology **26**, 1373 (2008).
- [10] S. S. Shevkopyas, T. Yoshida, L. L. Munn, and M. W. Bitensky, Analytical chemistry **77**, 933 (2005).
- [11] M. Kersaudy-Kerhoas and E. Sollier, Lab on a Chip **13**, 3323 (2013).
- [12] T.-R. Lee, M. Choi, A. M. Kopacz, S.-H. Yun, W. K. Liu, and P. Decuzzi, Scientific reports **3** (2013).
- [13] J. Tan, S. Shah, A. Thomas, H. D. Ou-Yang, and Y. Liu, Microfluidics and nanofluidics **14**, 77 (2013).
- [14] K. Müller, D. A. Fedosov, and G. Gompper, Scientific reports **4** (2014).
- [15] T.-R. Lee, M. S. Greene, Z. Jiang, A. M. Kopacz, P. Decuzzi, W. Chen, and W. K. Liu, Biomechanics and modeling in mechanobiology **13**, 515 (2014).
- [16] T.-R. Lee, S. S. Yoo, and J. Yang, Biomechanics and Modeling in Mechanobiology , 1 (2016).
- [17] J. Tan, W. Keller, S. Sohrabi, J. Yang, and Y. Liu, Nanomaterials **6**, 30 (2016).
- [18] R. D’Apolito, F. Taraballi, S. Minardi, X. Liu, S. Caserta, A. Cevenini, E. Tasciotti, G. Tomaiuolo, and S. Guido, Medical engineering & physics **38**, 17 (2016).
- [19] G. Schmid-Schönbein, R. Skalak, S. Usami, and S. Chien, Microvascular research **19**, 18 (1980).
- [20] H. Lipowsky, S. Rofe, L. Tannenbaum, J. Firrell, S. Usami, and S. Chien, in *Microvascular Research*, Vol. 21 (ACADEMIC PRESS INC JNL-COMP SUBSCRIPTIONS 525 B ST, STE 1900, SAN DIEGO, CA 92101-4495, 1981) pp. 249–250.
- [21] B. Klitzman and P. C. Johnson, American Journal of Physiology-Heart and Circulatory Physiology **242**, H211 (1982).
- [22] G. Mchedlishvili and M. Varazashvili, Bulletin of Experimental Biology and Medicine **93**, 550 (1982).
- [23] B. M. Fenton, R. T. Carr, and G. R. Cokelet, Microvascular research **29**, 103 (1985).
- [24] A. Pries, K. Ley, M. Claassen, and P. Gaehtgens, Microvascular research **38**, 81 (1989).
- [25] A. R. Pries and T. W. Secomb, American Journal of Physiology-Heart and Circulatory Physiology **289**, H2657 (2005).
- [26] I. G. Gould and A. A. Linninger, Microcirculation **22**, 1 (2015).
- [27] R. Guibert, C. Fonta, and F. Plouraboué, Transport in porous media **83**, 171 (2010).
- [28] A. Pries, T. W. Secomb, and P. Gaehtgens, The American journal of physiology **269**, H1713 (1995).
- [29] L. Gagnon, S. Sakadžić, F. Lesage, E. T. Mandeville, Q. Fang, M. A. Yaseen, and D. A. Boas, Neurophotonics **2**, 015008 (2015).
- [30] J. Yang, Y. E. Pak, and T.-R. Lee, Microvascular Research **108**, 22 (2016).
- [31] C. D. Murray, The Journal of general physiology **9**, 835 (1926).
- [32] T. F. Sherman, The Journal of general physiology **78**, 431 (1981).
- [33] A. Pries, T. W. Secomb, and P. Gaehtgens, Cardiovascular research **32**, 654 (1996).
- [34] J. Yang and Y. Wang, International journal for numerical methods in biomedical engineering **29**, 515 (2013).
- [35] A. Pries, K. Ley, and P. Gaehtgens, American Journal of Physiology-Heart and Circulatory Physiology **251**, H1324 (1986).